

¹ **Critical transitions and the fragmenting of global forests**

² **Leonardo A. Saravia^{1 3}, Santiago R. Doyle¹, Ben Bond-Lamberty²**

³ 1. Instituto de Ciencias, Universidad Nacional de General Sarmiento, J.M. Gutierrez 1159 (1613), Los
⁴ Polvorines, Buenos Aires, Argentina.

⁵ 2. Pacific Northwest National Laboratory, Joint Global Change Research Institute at the University of
⁶ Maryland–College Park, 5825 University Research Court #3500, College Park, MD 20740, USA

⁷ 3. Corresponding author e-mail: lsaravia@ungs.edu.ar

⁸ **Keywords:** Forest fragmentation, early warning signals, percolation, power-laws, MODIS, critical transitions

⁹ **Running title:** Critical fragmentation in global forest

¹⁰ **Abstract**

¹¹ 1. Forests provide critical habitat for many species, essential ecosystem services, and are coupled to
¹² atmospheric dynamics through exchanges of energy, water and gases. One of the most important
¹³ changes produced in the biosphere is the replacement of forest areas with human dominated landscapes.
¹⁴ This usually leads to fragmentation, altering the sizes of patches, the structure and function of the
¹⁵ forest. Here we studied the distribution and dynamics of forest patch sizes at a global level, examining
¹⁶ signals of a critical transition from an unfragmented to a fragmented state.

¹⁷ 2. We used MODIS vegetation continuous field to estimate the forest patches at a global level and de-
¹⁸ fined wide regions of connected forest across continents and big islands. We search for critical phase
¹⁹ transitions, where the system state of the forest changes suddenly at a critical point in time; this
²⁰ implies an abrupt change in connectivity that causes an increased fragmentation level. We combined
²¹ five criteria to evaluate the closeness of the system to a fragmentation threshold, studying in particular
²² the distribution of forest patch sizes and the dynamics of the largest patch over the last sixteen years.

²³ 3. We found some necessary evidence that allows us to analyze fragmentation as a critical transition:
²⁴ all regions followed a power-law distribution over the fifteen years. We also found that the Philip-
²⁵ pines region probably went through a critical transition from a fragmented to an unfragmented state.
²⁶ Neotropical regions with the highest deforestation rates—South America, Southeast Asia, Africa—all
²⁷ met the criteria to be near a critical fragmentation threshold.

²⁸ 4. This implies that human pressures and climate forcings might trigger undesired effects of fragmentation,
²⁹ such as species loss and degradation of ecosystems services, in these regions. The simple criteria
³⁰ proposed here could be used as an early warning to estimate the distance to a fragmentation threshold
³¹ in forests around the globe.

³² Introduction

³³ Forests are one of the most important biomes on earth, providing habitat for a large proportion of species
³⁴ and contributing extensively to global biodiversity (Crowther et al., 2015). In the previous century human
³⁵ activities have influenced global bio-geochemical cycles (Bonan, 2008; Canfield, Glazer, & Falkowski, 2010),
³⁶ with one of the most dramatic changes being the replacement of 40% of Earth's formerly biodiverse land
³⁷ areas with landscapes that contain only a few species of crop plants, domestic animals and humans (J. A.
³⁸ Foley et al., 2011). These local changes have accumulated over time and now constitute a global forcing
³⁹ (Barnosky et al., 2012). Another global scale forcing that is tied to habitat destruction is fragmentation,
⁴⁰ which is defined as the division of a continuous habitat into separated portions that are smaller and more
⁴¹ isolated. Fragmentation produces multiple interwoven effects: reductions of biodiversity between 13% and
⁴² 75%, decreasing forest biomass, and changes in nutrient cycling (Haddad et al., 2015). The effects of
⁴³ fragmentation are not only important from an ecological point of view but also that of human activities, as
⁴⁴ ecosystem services are deeply influenced by the level of landscape fragmentation (Angelsen, 2010; Mitchell
⁴⁵ et al., 2015; Rudel et al., 2005).

⁴⁶ Ecosystems have complex interactions between species and present feedbacks at different levels of organiza-
⁴⁷ tion (Gilman, Urban, Tewksbury, Gilchrist, & Holt, 2010), and external forcings can produce abrupt changes
⁴⁸ from one state to another, called critical transitions (Scheffer et al., 2009). These abrupt state shifts cannot
⁴⁹ be linearly forecasted from past changes, and are thus difficult to predict and manage (Scheffer et al., 2009).
⁵⁰ Such 'critical' transitions have been detected mostly at local scales (S. R. Carpenter et al., 2011; Drake &
⁵¹ Griffen, 2010), but the accumulation of changes in local communities that overlap geographically can prop-
⁵² agate and theoretically cause an abrupt change of the entire system at larger scales (Barnosky et al., 2012).
⁵³ Coupled with the existence of global scale forcings, this implies the possibility that a critical transition could
⁵⁴ occur at a global scale (C. Folke et al., 2011; Rockstrom et al., 2009).

⁵⁵ Complex systems can experience two general classes of critical transitions (R V Solé, 2011). In so-called first
⁵⁶ order transitions, a catastrophic regime shift that is mostly irreversible occurs because of the existence of
⁵⁷ alternative stable states (Scheffer et al., 2001). This class of transitions is suspected to be present in a variety
⁵⁸ of ecosystems such as lakes, woodlands, coral reefs (Scheffer et al., 2001), semi-arid grasslands (Brandon T.
⁵⁹ Bestelmeyer et al., 2011), and fish populations (Vasilakopoulos & Marshall, 2015). They can be the result of
⁶⁰ positive feedback mechanisms (Villa Martín, Bonachela, Levin, & Muñoz, 2015); for example, fires in some
⁶¹ forest ecosystems were more likely to occur in previously burned areas than in unburned places (Kitzberger,
⁶² Aráoz, Gowda, Mermoz, & Morales, 2012).

63 The other class of critical transitions are continuous or second order transitions (Ricard V. Solé & Bas-
64 compte, 2006). In these cases, there is a narrow region where the system suddenly changes from one domain
65 to another, with the change being continuous and in theory reversible. This kind of transitions were sug-
66 gested to be present in tropical forests (S. Pueyo et al., 2010), semi-arid mountain ecosystems (McKenzie
67 & Kennedy, 2012), and tundra shrublands (Naito & Cairns, 2015). The transition happens at a critical
68 point where we can observe a distinctive spatial pattern: scale invariant fractal structures characterized by
69 power law patch distributions (Stauffer & Aharony, 1994). There are several processes that can convert a
70 catastrophic transition to a second order transitions (Villa Martín et al., 2015). These include stochasticity,
71 such as demographic fluctuations, spatial heterogeneities, and/or dispersal limitation. All these components
72 are present in forest around the globe (Filotas et al., 2014; Fung, O'Dwyer, Rahman, Fletcher, & Chisholm,
73 2016; Seidler & Plotkin, 2006), and thus continuous transitions might be more probable than catastrophic
74 transitions. Moreover there is some evidence of recovery in some systems that supposedly suffered an irre-
75 versible transition produced by overgrazing (Brandon T Bestelmeyer, Duniway, James, Burkett, & Havstad,
76 2013; J. Y. Zhang, Wang, Zhao, Xie, & Zhang, 2005) and desertification (Allington & Valone, 2010).

77 The spatial phenomena observed in continuous critical transitions deal with connectivity, a fundamental
78 property of general systems and ecosystems from forests (Ochoa-Quintero, Gardner, Rosa, de Barros Ferraz,
79 & Sutherland, 2015) to marine ecosystems (Leibold & Norberg, 2004) and the whole biosphere (Lenton &
80 Williams, 2013). When a system goes from a fragmented to a connected state we say that it percolates (R
81 V Solé, 2011). Percolation implies that there is a path of connections that involves the whole system. Thus
82 we can characterize two domains or phases: one dominated by short-range interactions where information
83 cannot spread, and another in which long range interactions are possible and information can spread over
84 the whole area. (The term “information” is used in a broad sense and can represent species dispersal or
85 movement.) Thus, there is a critical “percolation threshold” between the two phases, and the system could
86 be driven close to or beyond this point by an external force; climate change and deforestation are the main
87 forces that could be the drivers of such a phase change in contemporary forests (Bonan, 2008; Haddad et al.,
88 2015). There are several applications of this concept in ecology: species’ dispersal strategies are influenced by
89 percolation thresholds in three-dimensional forest structure (Ricard V Solé, Bartumeus, & Gamarra, 2005),
90 and it has been shown that species distributions also have percolation thresholds (He & Hubbell, 2003).
91 This implies that pushing the system below the percolation threshold could produce a biodiversity collapse
92 (J. Bascompte & Solé, 1996; Pardini, Bueno, Gardner, Prado, & Metzger, 2010; Ricard V. Solé, Alonso, &
93 Saldaña, 2004); conversely, being in a connected state (above the threshold) could accelerate the invasion of
94 forest into prairie (Loehle, Li, & Sundell, 1996; Naito & Cairns, 2015).

95 One of the main challenges with systems that can experience critical transitions—of any kind—is that the
96 value of the critical threshold is not known in advance. In addition, because near the critical point a small
97 change can precipitate a state shift of the system, they are difficult to predict. Several methods have been
98 developed to detect if a system is close to the critical point, e.g. a deceleration in recovery from perturbations,
99 or an increase in variance in the spatial or temporal pattern (Boettiger & Hastings, 2012; S. R. Carpenter
100 et al., 2011; Dai, Vorselen, Korolev, & Gore, 2012; Hastings & Wysham, 2010).

101 The existence of a critical transition between two states has been established for forest at global scale in
102 different works (Hirotा, Holmgren, Nes, & Scheffer (2011); Verbesselt et al. (2016); Staal, Dekker, Xu, &
103 Nes (2016); Wuyts, Champneys, & House (2017)). It is generally believed that this constitutes a first order
104 catastrophic transition. The regions where forest can grow are not distributed homogeneously, as there
105 are demographic fluctuations in forest growth and disturbances produced by human activities. Due to new
106 theoretical advances (Villa Martín, Bonachela, & Muñoz, 2014; Villa Martín et al., 2015) all these factors
107 imply that if these were first order transitions they will be converted or observed as second order continuous
108 transitions. From this basis we applied indices derived from second order transitions to global forest cover
109 dynamics.

110 In this study, our objective is to look for evidence that forests around the globe are near continuous critical
111 points that represent a fragmentation threshold. We use the framework of percolation to first evaluate if
112 forest patch distribution at a continental scale is described by a power law distribution and then examine
113 the fluctuations of the largest patch. The advantage of using data at a continental scale is that for very
114 large systems the transitions are very sharp (R V Solé, 2011) and thus much easier to detect than at smaller
115 scales, where noise can mask the signals of the transition.

116 Methods

117 Study areas definition

118 We analyzed mainland forests at a continental scale, covering the whole globe, by delimiting land areas with
119 a near-contiguous forest cover, separated with each other by large non-forested areas. Using this criterion,
120 we delimited the following forest regions. In America, three regions were defined: South America temperate
121 forest (SAT), subtropical and tropical forest up to Mexico (SAST), and USA and Canada forest (NA). Europe
122 and North Asia were treated as one region (EUAS). The rest of the delimited regions were South-east Asia
123 (SEAS), Africa (AF), and Australia (OC). We also included in the analysis islands larger than 10^5 km^2 . The
124 mainland region has the number 1 e.g. OC1, and the nearby islands have consecutive numeration (Appendix

125 S4, figure S1-S6). We applied this criterion to delimit regions because we based our study on percolation
126 theory that assumes some kind of connectivity in the study area (see below).

127 **Forest patch distribution**

128 We studied forest patch distribution in each defined area from 2000 to 2015 using the MODerate-resolution
129 Imaging Spectroradiometer (MODIS) Vegetation Continuous Fields (VCF) Tree Cover dataset version 051
130 (C. DiMiceli et al., 2015). This dataset is produced at a global level with a 231-m resolution, from 2000
131 onwards on an annual basis. The last available MODIS year was 2015; for the region of Eurasia, we used
132 data only up to 2014 because of potential XXX errors (LEO - NEED TO BE MORE PRECISE ABOUT
133 WHAT “ERRORS”). There are several definition of forest based on percent tree cover (J. O. Sexton et al.,
134 2015); we choose a range from 20% to 30% threshold in 5% increments to convert the percentage tree cover
135 to a binary image of forest and non-forest pixels. This range is centered in the definition used by the United
136 Nations’ International Geosphere-Biosphere Programme (Belward, 1996), and studies of global fragmentation
137 (Haddad et al., 2015) and includes the range used in other studies of critical transitions (Xu et al., 2016).
138 Using this range we try to avoid the errors produced by low discrimination of MODIS VCF between forest
139 and dense herbaceous vegetation at low forest cover and the saturation of MODIS VCF in dense forests (J.
140 O. Sexton et al., 2013). We repeat all the analysis for this set of thresholds, except in some specific cases
141 described below. Patches of contiguous forest were determined in the binary image by grouping connected
142 forest pixels using a neighborhood of 8 forest units (Moore neighborhood). The MODIS VCF product defines
143 the percentage of tree cover by pixel, but does not discriminate the type of trees so besides natural forest it
144 includes plantations of tree crops like rubber, oil palm, eucalyptus and other managed stands (M. Hansen
145 et al., 2014).

146 **Percolation theory**

147 A more in-depth introduction to percolation theory can be found elsewhere (Stauffer & Aharony, 1994) and
148 a review from an ecological point of view is available (B. Oborny, Szabó, & Meszéna, 2007). Here, to explain
149 the basic elements of percolation theory we formulate a simple model: we represent our area of interest by a
150 square lattice and each site of the lattice can be occupied—e.g. by forest—with a probability p . The lattice
151 will be more occupied when p is greater, but the sites are randomly distributed. We are interested in the
152 connection between sites, so we define a neighborhood as the eight adjacent sites surrounding any particular
153 site. The sites that are neighbors of other occupied sites define a patch. When there is a patch that connects

154 the lattice from opposite sides, it is said that the system percolates. When p is increased from low values, a
155 percolating patch suddenly appears at some value of p called the critical point p_c .

156 Thus percolation is characterized by two well defined phases: the unconnected phase when $p < p_c$ (called
157 subcritical in physics), in which species cannot travel far inside the forest, as it is fragmented; in a general
158 sense, information cannot spread. The second is the connected phase when $p > p_c$ (supercritical), species
159 can move inside a forest patch from side to side of the area (lattice), i.e. information can spread over the
160 whole area. Near the critical point several scaling laws arise: the structure of the patch that spans the area
161 is fractal, the size distribution of the patches is power-law, and other quantities also follow power-law scaling
162 (Stauffer & Aharony, 1994).

163 The value of the critical point p_c depends on the geometry of the lattice and on the definition of the
164 neighborhood, but other power-law exponents only depend on the lattice dimension. Close to the critical
165 point, the distribution of patch sizes is:

166 (1) $n_s(p_c) \propto s^{-\alpha}$

167 where $n_s(p)$ is the number of patches of size s . The exponent α does not depend on the details of the
168 model and it is called universal (Stauffer & Aharony, 1994). These scaling laws can be applied for landscape
169 structures that are approximately random, or at least only correlated over short distances (Gastner, Oborny,
170 Zimmermann, & Pruessner, 2009). In physics this is called “isotropic percolation universality class”, and
171 corresponds to an exponent $\alpha = 2.05495$. If we observe that the patch size distribution has another exponent
172 it will not belong to this universality class and some other mechanism should be invoked to explain it.
173 Percolation thresholds can also be generated by models that have some kind of memory (Hinrichsen, 2000;
174 Ódor, 2004): for example, a patch that has been exploited for many years will recover differently than a
175 recently deforested forest patch. In this case, the system could belong to a different universality class, or in
176 some cases there is no universality, in which case the value of α will depend on the parameters and details
177 of the model (Corrado, Cherubini, & Pennetta, 2014).

178 To illustrate these concepts, we conducted simulations with a simple forest model with only two states: forest
179 and non-forest. This type of model is called a “contact process” and was introduced for epidemics (Harris,
180 1974), but has many applications in ecology (Gastner et al., 2009; Ricard V. Solé & Bascompte, 2006). A
181 site with forest can become extinct with probability e , and produce another forest site in a neighborhood
182 with probability c . We use a neighborhood defined by an isotropic power law probability distribution. We
183 defined a single control parameter as $\lambda = c/e$ and ran simulations for the subcritical fragmentation state
184 $\lambda < \lambda_c$, with $\lambda = 2$, near the critical point for $\lambda = 2.5$, and for the supercritical state with $\lambda = 5$ (see

185 supplementary data, gif animations).

186 **Patch size distributions**

187 We fitted the empirical distribution of forest patches calculated for each of the thresholds on the range
188 we previously mentioned. We used maximum likelihood (Clauset, Shalizi, & Newman, 2009; Goldstein,
189 Morris, & Yen, 2004) to fit four distributions: power-law, power-law with exponential cut-off, log-normal,
190 and exponential. We assumed that the patch size distribution is a continuous variable that was discretized
191 by the remote sensing data acquisition procedure.

192 We set a minimal patch size (X_{min}) at nine pixels to fit the patch size distributions to avoid artifacts at patch
193 edges due to discretization (Weerman et al., 2012). Besides this hard X_{min} limit we set due to discretization,
194 the power-law distribution needs a lower bound for its scaling behavior. This lower bound is also estimated
195 from the data by maximizing the Kolmogorov-Smirnov (KS) statistic, computed by comparing the empirical
196 and fitted cumulative distribution functions (Clauset et al., 2009). For the log-normal model we constrain
197 the values of the μ parameter to positive values, this parameter controls the mode of the distribution and
198 when is negative most of the probability density of the distribution lies outside the range of the forest patch
199 size data (Limpert, Stahel, & Abbt, 2001).

200 To select the best model we calculated corrected Akaike Information Criteria (AIC_c) and Akaike weights for
201 each model (Burnham & Anderson, 2002). Akaike weights (w_i) are the weight of evidence in favor of model
202 i being the actual best model given that one of the N models must be the best model for that set of N
203 models. Additionally, we computed a likelihood ratio test (Clauset et al., 2009; Vuong, 1989) of the power
204 law model against the other distributions. We calculated bootstrapped 95% confidence intervals (Crawley,
205 2012) for the parameters of the best model, using the bias-corrected and accelerated (BCa) bootstrap (Efron
206 & Tibshirani, 1994) with 10000 replications.

207 **Largest patch dynamics**

208 The largest patch is the one that connects the highest number of sites in the area. This has been used
209 extensively to indicate fragmentation (R. H. Gardner & Urban, 2007; Ochoa-Quintero et al., 2015). The
210 relation of the size of the largest patch S_{max} to critical transitions has been extensively studied in relation to
211 percolation phenomena (Bazant, 2000; Botet & Ploszajczak, 2004; Stauffer & Aharony, 1994), but is seldom
212 used in ecological studies (for an exception see Gastner et al. (2009)). When the system is in a connected
213 state ($p > p_c$) the landscape is almost insensitive to the loss of a small fraction of forest, but close to the

214 critical point a minor loss can have important effects (B. Oborny et al., 2007; Ricard V. Solé & Bascompte,
215 2006), because at this point the largest patch will have a filamentary structure, i.e. extended forest areas
216 will be connected by thin threads. Small losses can thus produce large fluctuations.

217 One way to evaluate the fragmentation of the forest is to calculate the proportion of the largest patch
218 against the total area (T. H. Keitt, Urban, & Milne, 1997). The total area of the regions we are considering
219 (Appendix S4, figures S1-S6) may not be the same than the total area that the forest could potentially occupy,
220 and thus a more accurate way to evaluate the weight of S_{max} is to use the total forest area, which can be
221 easily calculated by summing all the forest pixels. We calculate the proportion of the largest patch for each
222 year, dividing S_{max} by the total forest area of the same year: $RS_{max} = S_{max} / \sum_i S_i$. This has the effect of
223 reducing the S_{max} fluctuations produced due to environmental or climatic changes influences in total forest
224 area. When the proportion RS_{max} is large (more than 60%) the largest patch contains most of the forest so
225 there are fewer small forest patches and the system is probably in a connected phase. Conversely, when it is
226 low (less than 20%), the system is probably in a fragmented phase (Saravia & Momo, 2017). To define if a
227 region will be in a connected or unconnected state we used the RS_{max} of the highest (i.e., most conservative)
228 threshold of 40%, that represent the most dense area of forest within our chosen range. We assume that
229 there are two alternative states for the critical transition—the forest could be fragmented or unfragmented.
230 If RS_{max} is a good indicator of the fragmentation state of the forest its distribution of frequencies should be
231 bimodal (Brandon T. Bestelmeyer et al., 2011), so we apply the Hartigan's dip test that measures departures
232 from unimodality (J. A. Hartigan & Hartigan, 1985).

233 The RS_{max} is a useful qualitative index that does not tell us if the system is near or far from the critical
234 transition; this can be evaluated using the temporal fluctuations. We calculate the fluctuations around the
235 mean with the absolute values $\Delta S_{max} = S_{max}(t) - \langle S_{max} \rangle$, using the proportions of RS_{max} . To characterize
236 fluctuations we fitted three empirical distributions: power-law, log-normal, and exponential, using the same
237 methods described previously. We expect that large fluctuation near a critical point have heavy tails (log-
238 normal or power-law) and that fluctuations far from a critical point have exponential tails, corresponding to
239 Gaussian processes (Rooij, Nash, Rajaraman, & Holden, 2013). As the data set spans 16 years, it is probable
240 that will do not have enough power to reliably detect which distribution is better (Clauset et al., 2009). To
241 improve this we used the same likelihood ratio test we used previously (Clauset et al., 2009; Vuong, 1989);
242 if the p-value obtained to compare the best distribution against the others we concluded that there is not
243 enough data to decide which is the best model. We generated animated maps showing the fluctuations of
244 the two largest patches at 30% threshold, to aid in the interpretations of the results.

245 A robust way to detect if the system is near a critical transition is to analyze the increase in variance of the

246 density (Benedetti-Cecchi, Tamburello, Maggi, & Bulleri, 2015). It has been demonstrated that the variance
247 increase in density appears when the system is very close to the transition (Corrado et al., 2014), and thus
248 practically it does not constitute an early warning indicator. An alternative is to analyze the variance of
249 the fluctuations of the largest patch ΔS_{max} : the maximum is attained at the critical point but a significant
250 increase occurs well before the system reaches the critical point (Corrado et al., 2014; Saravia & Momo,
251 2017). In addition, before the critical fragmentation, the skewness of the distribution of ΔS_{max} should be
252 negative, implying that fluctuations below the average are more frequent. We characterized the increase in
253 the variance using quantile regression: if variance is increasing the slopes of upper or/and lower quartiles
254 should be positive or negative.

255 All statistical analyses were performed using the GNU R version 3.3.0 (R Core Team, 2015), to fit the
256 distributions of patch sizes we used the Python package powerlaw (Alstott, Bullmore, & Plenz, 2014). For
257 the quantile regressions we used the R package quantreg (Koenker, 2016). Image processing was done
258 in MATLAB r2015b (The Mathworks Inc.). The complete source code for image processing and statistical
259 analysis, and the patch size data files are available at figshare <http://dx.doi.org/10.6084/m9.figshare.4263905>.

260 Results

261 The figure 1 shows an example of the distribution of the biggest 200 patches for years 2000 and 2014. This
262 distribution is highly variable; the biggest patch usually maintains its spatial location, but sometimes it
263 breaks and then big fluctuations in its size are observed, as we will analyze below. Smaller patches can
264 merge or break more easily so they enter or leave the list of 200, and this is why there is a color change
265 across years.

266 The power law distribution was selected as the best model in 99% of the cases (Figure S7). In a small
267 number of cases (1%) the power law with exponential cutoff was selected, but the value of the parameter α
268 was similar by ± 0.03 to the pure power law (Table S1, and model fit data table). Additionally the patch size
269 where the exponential tail begins is very large, and thus we used the power law parameters for these cases
270 (region EUAS3,SAST2). In finite-size systems the favored model should be the power law with exponential
271 cut-off, because the power-law tails are truncated to the size of the system (Stauffer & Aharony, 1994). This
272 implies that differences between the two kinds of power law models should be small. We observe this effect:
273 when the pure power-law model is selected as the best model the likelihood ratio test shows that in 64% of
274 the cases the differences with power law with exponential cutoff are not significant ($p\text{-value}>0.05$); in these
275 cases the differences between the fitted α for both models are less than 0.001. Instead the likelihood ratio

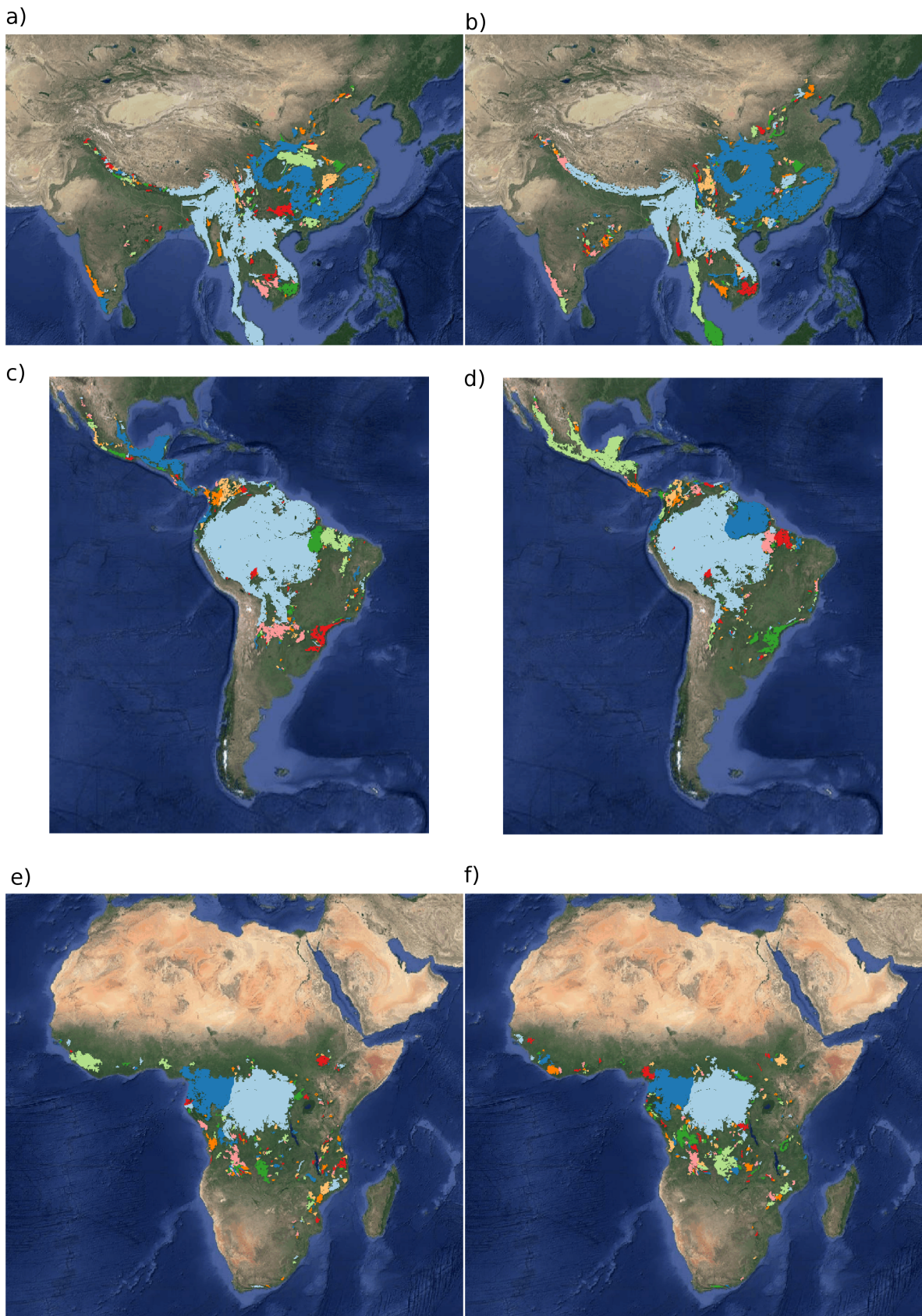


Figure 1: Forest patch distributions for continental regions for the years 2000 and 2014. The images are the 200 biggest patches, shown at a coarse pixel scale of 2.5 km. The regions are: a) & b) southeast Asia; c) & d) South America subtropical and tropical and e) & f) Africa mainland, for the years 2000 and 2014 respectively. The color palette was chosen to discriminate different patches and does not represent patch size.

276 test clearly differentiates the power law model from the exponential model (100% cases p-value<0.05), and
277 the log-normal model (90% cases p-value<0.05).

278 The global mean of the power-law exponent α is 1.967 and the bootstrapped 95% confidence interval is
279 1.964 - 1.970. The global values for each threshold are different, because their confidence intervals do not
280 overlap, and their range goes from 1.90 to 2.01 (Table S1). Analyzing the biggest regions (Figure 1, Table
281 S2) the northern hemisphere regions (EUAS1 & NA1) have similar values of α (1.97, 1.98), pantropical areas
282 have different α with greatest values for South America (SAST1, 2.01) and in descending order Africa (AF1,
283 1.946) and Southeast Asia (SEAS1, 1.895). With greater α the fluctuations of patch sizes are lower and vice
284 versa (M. E. J. Newman, 2005).

285 We calculated the total areas of forest and the largest patch S_{max} by year for different thresholds, and as
286 expected these two values increase for smaller thresholds (Table S3). We expect fewer variations in the
287 largest patch relative to total forest area RS_{max} (Figure S9); in ten cases it stayed near or higher than 60%
288 (EUAS2, NA5, OC2, OC3, OC4, OC5, OC6, OC8, SAST1, SAT1) over the 25-35 range or more. In four
289 cases it stayed around 40% or less, at least over the 25-30% range (AF1, EUAS3, OC1, SAST2), and in six
290 cases there is a crossover from more than 60% to around 40% or less (AF2, EUAS1, NA1, OC7, SEAS1,
291 SEAS2). This confirms the criteria of using the most conservative threshold value of 40% to interpret RS_{max}
292 with regard to the fragmentation state of the forest. The frequency of RS_{max} showed bimodality (Figure 3)
293 and the dip test rejected unimodality ($D = 0.0416$, p-value = 0.0003), which also implies that RS_{max} is a
294 good index to study the fragmentation state of the forest.

295 The RS_{max} for regions with more than 10^7 km² of forest is shown in figure 4. South America tropical and
296 subtropical (SAST1) is the only region with an average close to 60%, the other regions are below 30%. Eurasia
297 mainland (EUAS1) has the lowest value near 20%. For regions with less total forest area (Figure S10, Table
298 S3), Great Britain (EUAS3) has the lowest proportion less than 5%, Java (OC7) and Cuba (SAST2) are
299 under 25%, while other regions such as New Guinea (OC2), Malaysia/Kalimantan (OC3), Sumatra (OC4),
300 Sulawesi (OC5) and South New Zealand (OC6) have a very high proportion (75% or more). Philippines
301 (SEAS2) seems to be a very interesting case because it seems to be under 30% until the year 2007, fluctuates
302 around 30% in years 2008-2010, then jumps near 60% in 2011-2013 and then falls again to 30%, this seems
303 an example of a transition from a fragmented state to a unfragmented one (figure S10).

304 We analyzed the distributions of fluctuations of the largest patch relative to total forest area ΔRS_{max} and
305 the fluctuations of the largest patch ΔS_{max} . Although the Akaike criteria identified different distributions
306 as the best, in most cases the Likelihood ratio test was not significant and we are not able, from these data,

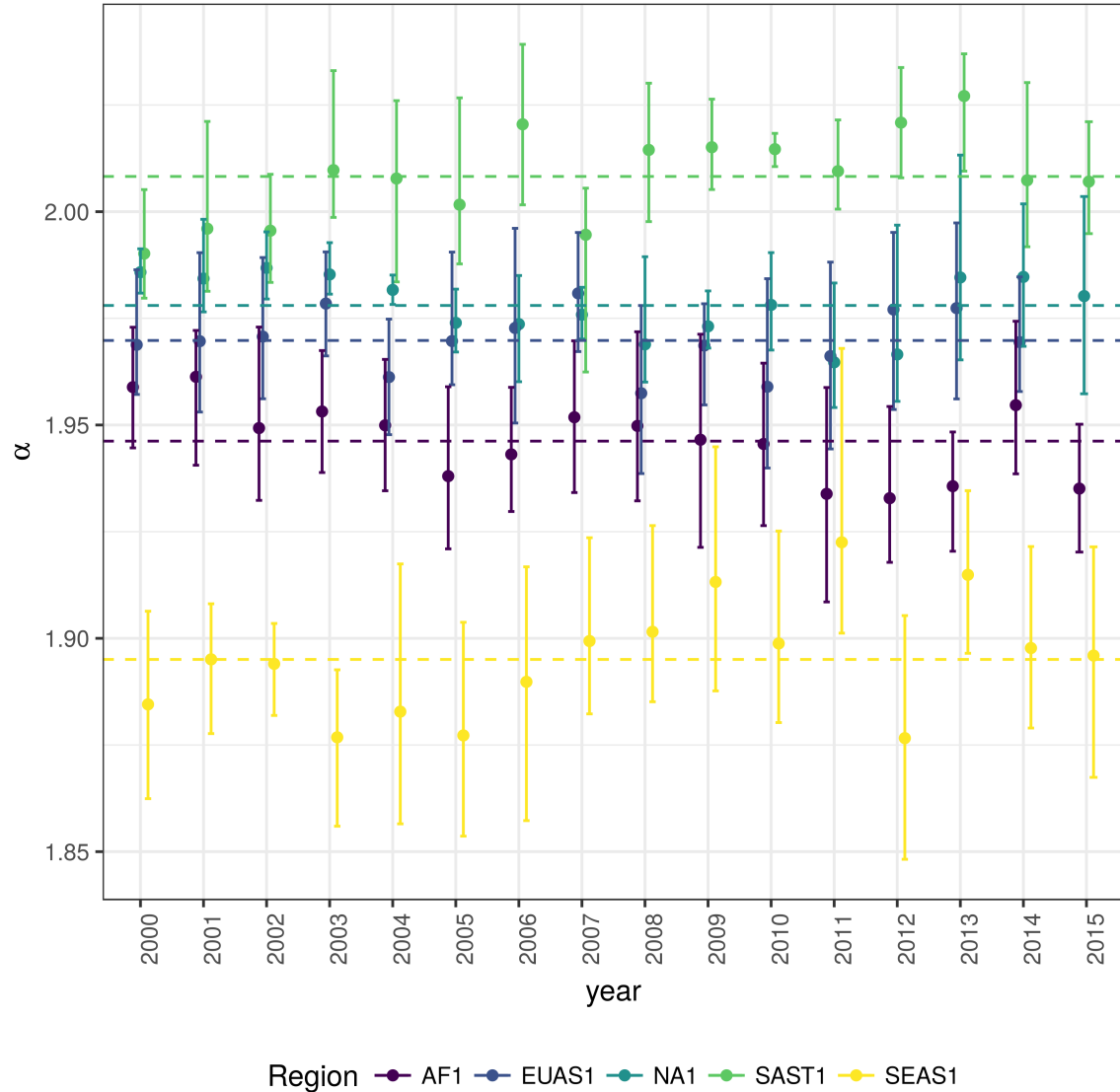


Figure 2: Power law exponents (α) of forest patch distributions for regions with total forest area $> 10^7 \text{ km}^2$. Dashed horizontal lines are the means by region, with 95% confidence interval error bars estimated by bootstrap resampling. The regions are AF1: Africa mainland, EUAS1: Eurasia mainland, NA1: North America mainland, SAST1: South America subtropical and tropical, SEAS1: Southeast Asia mainland.

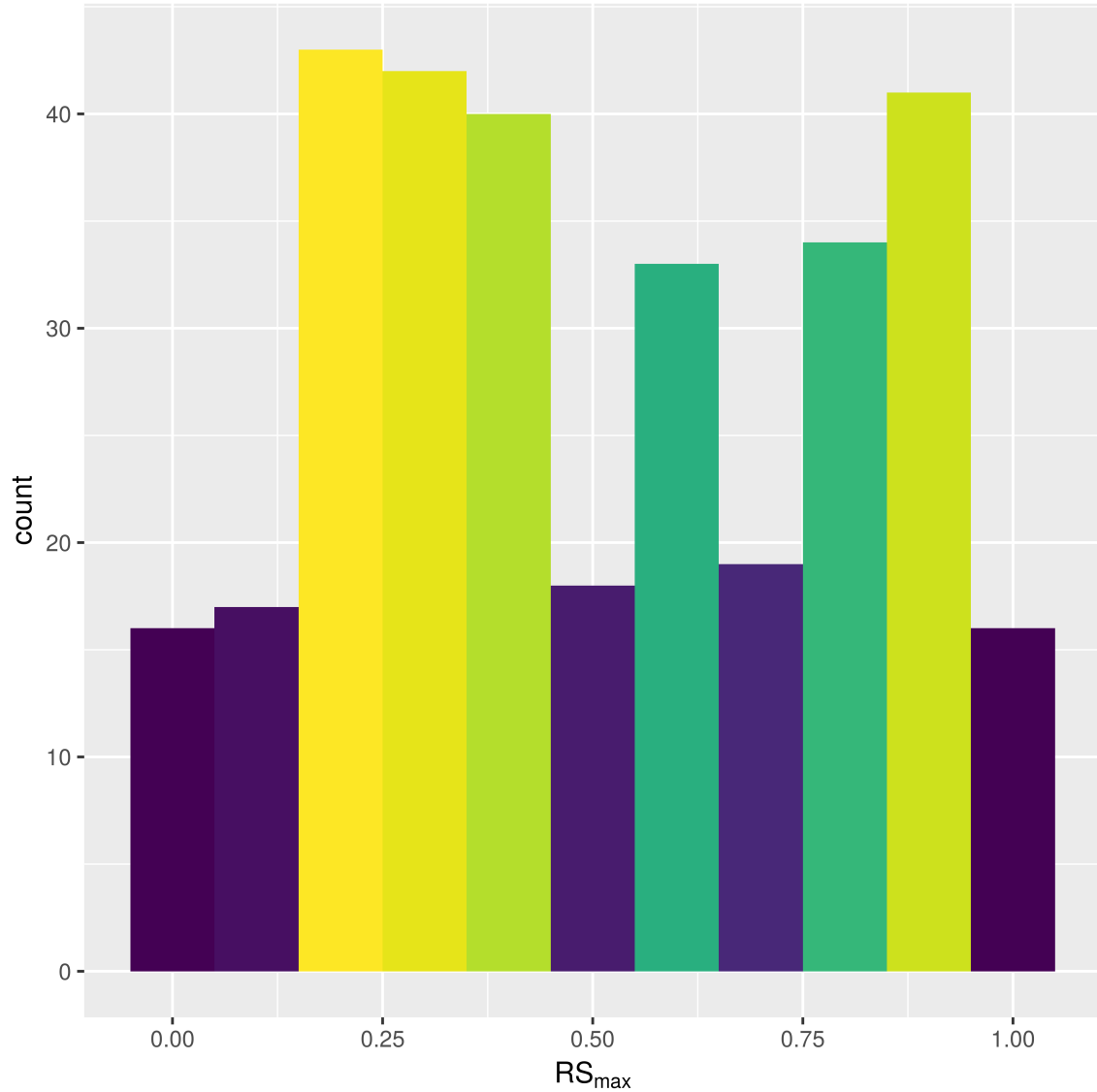


Figure 3: Frequency distribution of Largest patch proportion relative to total forest area RS_{max} calculated using a threshold of 40% of forest in each pixel to determine patches. Bimodality is observed and confirmed by the dip test ($D = 0.0416$, $p\text{-value} = 0.0003$). This indicates the existence of two states needed for a critical transition.

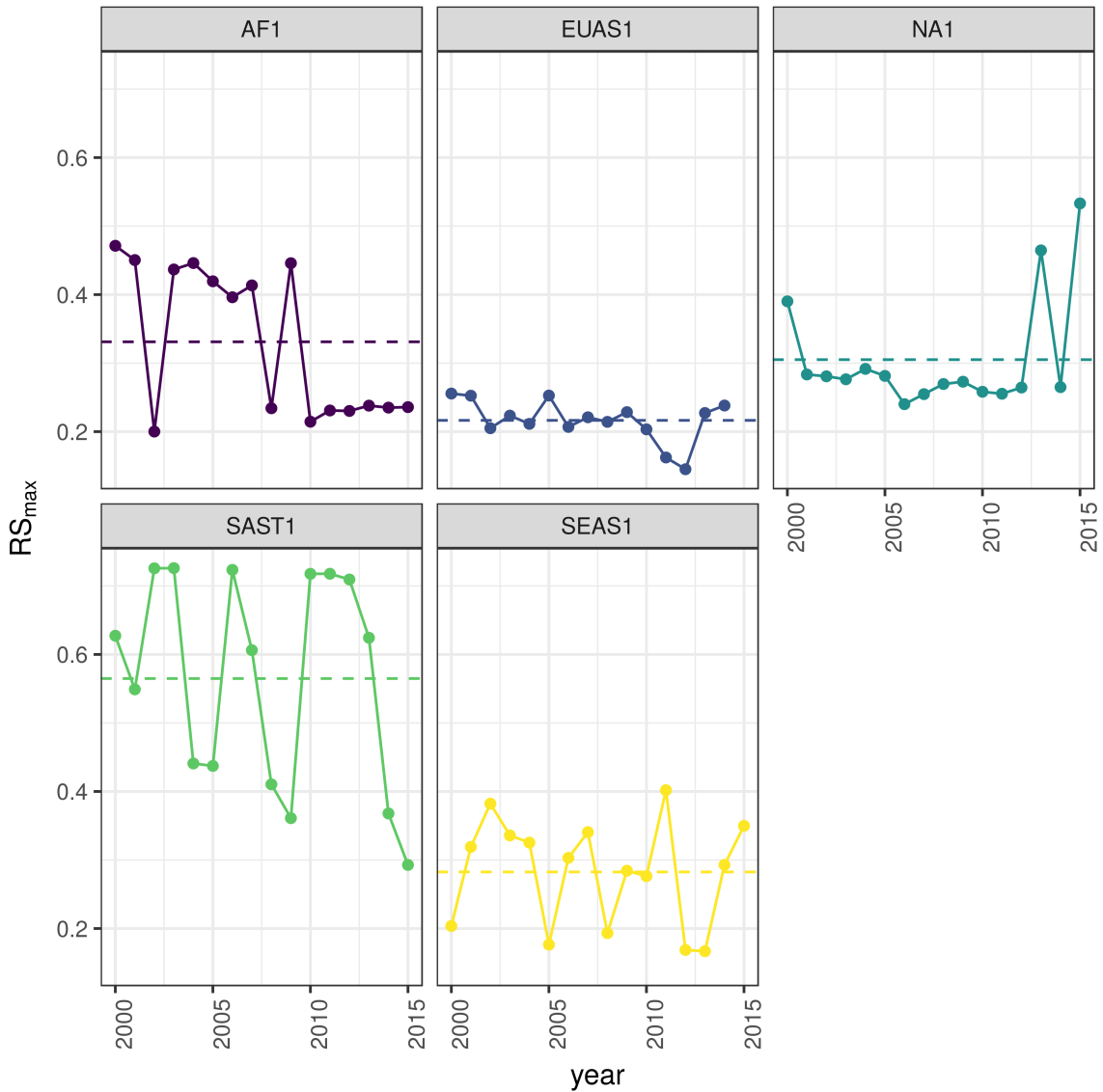


Figure 4: Largest patch proportion relative to total forest area RS_{max} , for regions with total forest area $> 10^7 \text{ km}^2$. We show here the RS_{max} calculated using a threshold of 40% of forest in each pixel to determine patches. Dashed lines are averages across time. The regions are AF1: Africa mainland, EUAS1: Eurasia mainland, NA1: North America mainland, SAST1: South America tropical and subtropical, SEAS1: Southeast Asia mainland.

307 to determine with confidence which is the best distribution. In only one case was the distribution selected
308 by the Akaike criteria confirmed as the correct model for relative and absolute fluctuations (Table S4).

309 The animations of the two largest patches (see supplementary data, largest patch gif animations) qualitatively
310 shows the nature of fluctuations and if the state of the forest is connected or not. If the largest patch is
311 always the same patch over time, the forest is probably not fragmented; this happens for regions with RS_{max}
312 of more than 40% such as AF2 (Madagascar), EUAS2 (Japan), NA5 (Newfoundland) and OC3 (Malaysia).
313 In regions with RS_{max} between 40% and 30% the identity of the largest patch could change or stay the same
314 in time. For OC7 (Java) the largest patch changes and for AF1 (Africa mainland) it stays the same. Only for
315 EUAS1 (Eurasia mainland) did we observe that the two largest patches are always the same, implying that
316 this region is probably composed of two independent domains and should be sub-divided in future studies.
317 The regions with RS_{max} less than 25% included SAST2 (Cuba) and EUAS3 (Great Britain); in these cases
318 the always-changing largest patch reflects their fragmented state. In the case of SEAS2 (Philippines) a
319 transition is observed, with the identity of the largest patch first variable, and then constant after 2010.

320 The results of quantile regressions are almost identical for ΔRS_{max} and ΔS_{max} (table S5). Among the biggest
321 regions, Africa (AF1) has a similar pattern across thresholds but only the 30% threshold is significant; the
322 upper and lower quantiles have significant negative slopes, but the lower quantile slope is lower, implying
323 that negative fluctuations and variance are increasing (Figure 5). Eurasia mainland (EUAS1) has significant
324 slopes at 20%, 30% and 40% thresholds but the patterns are different at 20% variance is decreasing, at
325 30% and 40% only is increasing. Thus the variation of the most dense portion of the largest patch is
326 increasing within a limited range. North America mainland (NA1) exhibits the same pattern at 20%, 25%
327 and 30% thresholds: a significant lower quantile with positive slope, implying decreasing variance. South
328 America tropical and subtropical (SAST1) have significant lower quantile with negative slope at 25% and 30%
329 thresholds indicating an increase in variance. SEAS1 has an upper quantile with positive slope significant
330 for 25% threshold, also indicating an increasing variance. The other regions, with forest area smaller than
331 10^7 km^2 are shown in figure S11 and table S5. Philippines (SEAS2) is an interesting case: the slopes of lower
332 quantiles are positive for thresholds 20% and 25%, and the upper quantile slopes are positive for thresholds
333 30% and 40%; thus variance is decreasing at 20%-25% and increasing at 30%-40%.

334 The conditions that indicate that a region is near a critical fragmentation threshold are that patch size
335 distributions follow a power law; variance of ΔRS_{max} is increasing in time; and skewness is negative. All
336 these conditions must happen at the same time at least for one threshold. When the threshold is higher more
337 dense regions of the forest are at risk. This happens for Africa mainland (AF1), Eurasia mainland(EUAS1),
338 Japan (EUAS2), Australia mainland (OC1), Malaysia/Kalimantan (OC3), Sumatra (OC4), South America

339 tropical & subtropical (SAST1), Cuba (SAST2), Southeast Asia, Mainland (SEAS1).

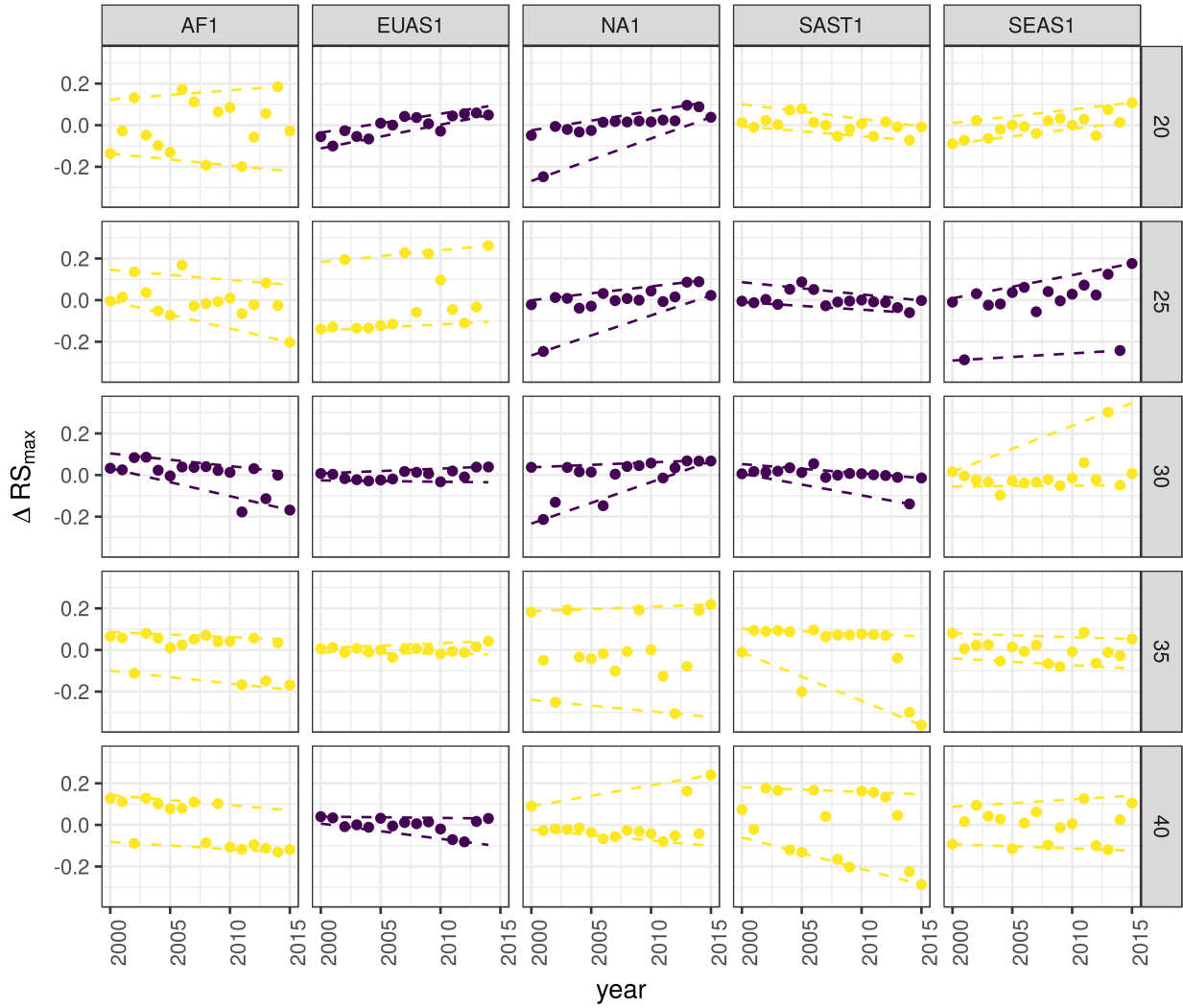


Figure 5: Largest patch fluctuations for regions with total forest area $> 10^7 \text{ km}^2$ across years. The patch sizes are relative to the total forest area of the same year. Dashed lines are 90% and 10% quantile regressions, to show if fluctuations were increasing; purple (dark) panels have significant slopes. The regions are AF1: Africa mainland, EUAS1: Eurasia mainland, NA1: North America mainland, SAST1: South America tropical and subtropical, SEAS1: Southeast Asia mainland.

Table 1: Regions and indicators of closeness to a critical fragmentation point. Where: RS_{max} is the largest patch divided by the total forest area; Threshold is the value used to calculate patches from the MODIS VCF pixels; ΔRS_{max} are the fluctuations of RS_{max} around the mean and the increase or decrease in the variance was estimated using quantile regressions; skewness was calculated for RS_{max} . NS means the results were non-significant. The conditions that determine the closeness to a fragmentation point are: increasing variance of ΔRS_{max} and negative skewness. RS_{max} indicates if the forest is unfragmented (>0.6) or fragmented (<0.3).

Region	Description	RS_{max}	Threshold	Variance of ΔRS_{max}	Skewness
AF1	Africa mainland	0.33	30	Increase	-1.4653
AF2	Madagascar	0.48	20	Increase	0.7226
EUAS1	Eurasia, mainland	0.22	20	Decrease	-0.4814
EUAS1			30	Increase	0.3113
EUAS1			40	Increase	-1.2790
EUAS2	Japan	0.94	35	Increase	-0.3913
EUAS2			40	Increase	-0.5030
EUAS3	Great Britain	0.03	40	NS	
NA1	North America, mainland	0.31	20	Decrease	-2.2895
NA1			25	Decrease	-2.4465
NA1			30	Decrease	-1.6340
NA5	Newfoundland	0.54	40	NS	
OC1	Australia, Mainland	0.36	30	Increase	0.0920
OC1			35	Increase	-0.8033
OC2	New Guinea	0.96	25	Decrease	-0.1003
OC2			30	Decrease	0.1214
OC2			35	Decrease	-0.0124
OC3	Malaysia/Kalimantan	0.92	35	Increase	-1.0147
OC3			40	Increase	-1.5649
OC4	Sumatra	0.84	20	Increase	-1.3846
OC4			25	Increase	-0.5887
OC4			30	Increase	-1.4226
OC5	Sulawesi	0.82	40	NS	
OC6	New Zealand South Island	0.75	40	Increase	0.3553
OC7	Java	0.16	40	NS	
OC8	New Zealand North Island	0.64	40	NS	
SAST1	South America, Tropical and Subtropical forest	0.56	25	Increase	1.0519
SAST1			30	Increase	-2.7216
SAST2	Cuba	0.15	20	Increase	0.5049
SAST2			25	Increase	1.7263
SAST2			30	Increase	0.1665
SAST2			40	Increase	-0.5401
SAT1	South America, Temperate forest	0.54	25	Decrease	0.1483
SAT1			30	Decrease	-1.6059
SAT1			35	Decrease	-1.3809
SEAS1	Southeast Asia, Mainland	0.28	25	Increase	-1.3328
SEAS2	Philippines	0.33	20	Decrease	-1.6373
SEAS2			25	Decrease	-0.6648
SEAS2			30	Increase	0.1517

Region	Description	RS_{max}	Threshold	Variance of ΔRS_{max}	Skewness
SEAS2			40	Increase	1.5996

340 Discussion

341 We found that the forest patch distribution of all regions of the world, spanning tropical rainforests, boreal
 342 and temperate forests, followed power laws spanning seven orders of magnitude. Power laws have previously
 343 been found for several kinds of vegetation, but never at global scales as in this study. Moreover the range
 344 of the estimated power law exponents is relatively narrow (1.90 - 2.01), even though we tested a variety
 345 of different thresholds levels. This suggest the existence of one unifying mechanism, or perhaps different
 346 mechanisms that act in the same way in different regions, affecting forest spatial structure and dynamics.

347 Several mechanisms have been proposed for the emergence of power laws in forests. The first is related
 348 self organized criticality (SOC), when the system is driven by its internal dynamics to a critical state; this
 349 has been suggested mainly for fire-driven forests (Hantson, Pueyo, & Chuvieco, 2015; Zinck & Grimm,
 350 2009). Real ecosystems do not seem to meet the requirements of SOC dynamics (McKenzie & Kennedy,
 351 2012; S. Pueyo et al., 2010), however, because they have both endogenous and exogenous controls, are non-
 352 homogeneous, and do not have a separation of time scales [Ricard V Solé, Alonso, & Mckane (2002); Sole2006].

353 A second possible mechanism, suggested by Pueyo et al. (2010), is isotropic percolation: when a system is
 354 near the critical point, the power law structures arise. This is equivalent to the random forest model that
 355 we explained previously, and requires the tuning of an external environmental condition to carry the system
 356 to this point. We did not expect forest growth to be a random process at local scales, but it is possible that
 357 combinations of factors cancel out to produce seemingly random forest dynamics at large scales. In this case
 358 we should have observed power laws in a limited set of situations that coincide with a critical point, but
 359 instead we observed pervasive power law distributions. Thus isotopic percolation does not seem likely to be
 360 the mechanism that produces the observed distributions. A third possible mechanism is facilitation (Irvine,
 361 Bull, & Keeling, 2016; Manor & Shnerb, 2008): a patch surrounded by forest will have a smaller probability
 362 of being deforested or degraded than an isolated patch. The model of Scanlon et al. (2007) showed an
 363 $\alpha = 1.34$ which is different from our results (1.90 - 2.01 range). Another model but with three states
 364 (tree/non-tree/degraded), including local facilitation and grazing, was also used to obtain power laws patch
 365 distributions without external tuning, and exhibited deviations from power laws at high grazing pressures
 366 (S. Kéfi et al., 2007). The values of the power law exponent α obtained for this model are dependent on the
 367 intensity of facilitation: when facilitation is more intense the exponent is higher, but the maximal values they

368 obtained are still lower than the ones we observed. The interesting point is that the value of the exponent is
369 dependent on the parameters, and thus the observed α might be obtained with some parameter combination.

370 The existence of possible critical transitions in forests, mainly in neotropical forest to savanna, is a matter
371 of intense investigation, with the transitions generally thought to be first order or discontinuous transitions.

372 Here, however, we found power laws in forest patch distributions, implying (i.e., a necessary but not a
373 sufficient condition) a second order or continuous transition. A power law patch distribution can be indicative
374 of a critical transition if it is present in a narrow range of conditions; conversely, if it is not found, the existence
375 of a critical transition cannot be discarded. New research (Villa Martín et al., 2014, 2015) has suggested
376 that first order transitions do not even exist when the system is (i) spatially heterogeneous and (ii) exhibits
377 internal and external stochastic fluctuations, as in forests. Thus the application of indices based on second
378 order transitions seems to be justified.

379 It has been suggested that a combination of spatial and temporal indicators could more reliably detect
380 critical transitions (S. Kéfi et al., 2014). In this study, we combined five criteria to evaluate the closeness
381 of the system to a fragmentation threshold. Two of them were spatial: the forest patch size distribution,
382 and the proportion of the largest patch relative to total forest area RS_{max} . The other three were the
383 distribution of temporal fluctuations in the largest patch size, the trend in the variance, and the skewness
384 of the fluctuations. One of them: the distribution of temporal fluctuations ΔRS_{max} can not be applied
385 with our temporal resolution due to the difficulties of fitting and comparing heavy tailed distributions. The
386 combination of the remaining four gives us an increased degree of confidence about the system being close
387 to a critical transition.

388 Monitoring the biggest patches using RS_{max} is also important regardless of the existence or not of critical
389 transitions. RS_{max} is relative to total forest area thus it could be used to compare regions with a different
390 extension of forests and as the total area of forest also changes with different environmental conditions,
391 e.g. this could be used to compare forest from different latitudes. Moreover, the areas covered by S_{max}
392 across regions contain most of the intact forest landscapes defined by P. Potapov et al. (2008), and thus
393 RS_{max} is a relatively simple way to evaluate the risk in these areas.

394 This analysis is at scale of continents so it is in fact a macrosystems analysis (Heffernan et al., 2014), in
395 which it is important to link local processes with resulting larger-scale (here, continental) patterns. Here, we
396 identified macro-scale dynamical patterns that deserve attention. To link these patterns across scales requires
397 a substantial amount of investigation, probably performing the same analysis for smaller regions that identify
398 more clearly which kind of forest and processes are locally involved. We know that the same procedure could

399 be applied to local scales because the patch distributions are power laws; power law distributions are self-
400 similar, or invariant to scale changes. Thus unless power law distribution are broken we could apply the
401 same methodology to more local scales.

402 South America tropical and subtropical (SAST1), Southeast Asia mainland (SEAS1) and Africa mainland
403 (AF1) met all criteria at least for one threshold; these regions generally experience the biggest rates of
404 deforestation with a significant increase in loss of forest (M. C. Hansen et al., 2013). From our point of view
405 the most critical region is Southeast Asia, because the proportion of the largest patch relative to total forest
406 area RS_{max} was 28%. This suggests that Southeast Asia's forests are the most fragmented, and thus its
407 flora and fauna the most endangered. Due to the criteria we adopted to define regions, we could not detect
408 the effect of conservation policies applied at a country level, e.g. the Natural Forest Conservation Program
409 in China, which has produced an 1.6% increase in forest cover and net primary productivity over the last
410 20 years (Viña, McConnell, Yang, Xu, & Liu, 2016). Indonesia and Malaysia (OC3) both are countries with
411 hight deforestation rates (M. C. Hansen et al., 2013); Sumatra (OC4) is the biggest island of Indonesia and
412 where most deforestation occurs. Both regions show a high RS_{max} greater than 60%, and thus the forest is
413 in an unfragmented state, but they met all other criteria, meaning that they are approaching a transition if
414 the actual deforestation rates continue. At present our indices are qualitative but we expect to develop them
415 in a more quantitative way to predict how many years would be needed to complete a critical transition if
416 actual forest loss rates are maintained.

417 The Eurasian mainland region (EUAS1) is an extensive area with mainly temperate and boreal forest, and a
418 combination of forest loss due to fire (P. Potapov, Hansen, Stehman, Loveland, & Pittman, 2008) and forestry.
419 The biggest country is Russia that experienced the biggest rate of forest loss of all countries, but here in
420 the zone of coniferous forest the the largest gain is observed due to agricultural abandonment (Prishchepov,
421 Müller, Dubinin, Baumann, & Radeloff, 2013). The loss is maximum at the most dense areas of forest (M.
422 C. Hansen et al., 2013, Table S3), this coincides with our analysis that detect an increasing risk at denser
423 forest. This region also has a relatively low RS_{max} that means is probably near a fragmented state. A region
424 that is similar in forest composition to EAUS1 is North America (NA1); the two main countries involved,
425 United States and Canada, have forest dynamics mainly influenced by fire and forestry, with both regions are
426 extensively managed for industrial wood production. North America has a higher RS_{max} than Eurasia and
427 a positive skewness that excludes it from being near a critical transition. A possible explanation of this is
428 that in Russia after the collapse of the Soviet Union harvest was lower due to agricultural abandonment but
429 illegal overharvesting of high valued stands has increased in recent decades (Gauthier, Bernier, Kuuluvainen,
430 Shvidenko, & Schepaschenko, 2015).

431 The analysis of RS_{max} reveals that the island of Philippines (SEAS2) seems to be an example of a critical
432 transition from an unconnected to a connected state, i.e. from a state with high fluctuations and low RS_{max}
433 to a state with low fluctuations and high RS_{max} . If we observe this pattern backwards in time, the decrease
434 in variance increases, and negative skewness is constant, and thus the region exhibits the criteria of a critical
435 transition (Table 1, Figure S11). The actual pattern of transition to an unfragmented state could be the
436 result of an active intervention of the government promoting conservation and rehabilitation of protected
437 areas, ban of logging old-growth forest, reforestation of barren areas, community-based forestry activities,
438 and sustainable forest management in the country's production forest (Lasco et al., 2008). This confirms
439 that the early warning indicators proposed here work in the correct direction. An important caveat is that
440 the MODIS dataset does not detect if native forest is replaced by agroindustrial tree plantations like oil
441 palms, that are among the main drivers of deforestation in this area (Malhi, Gardner, Goldsmith, Silman, &
442 Zelazowski, 2014). To improve the estimation of forest patches, data sets as the MODIS cropland probability
443 and others about land use, protected areas, forest type, should be incorporated (M. Hansen et al., 2014; J.
444 O. Sexton et al., 2015).

445 Deforestation and fragmentation are closely related. At low levels of habitat reduction species population
446 will decline proportionally; this can happen even when the habitat fragments retain connectivity. As habitat
447 reduction continues, the critical threshold is approached and connectivity will have large fluctuations (Brook,
448 Ellis, Perring, Mackay, & Blomqvist, 2013). This could trigger several negative synergistic effects: population
449 fluctuations and the possibility of extinctions will rise, increasing patch isolation and decreasing connectivity
450 (Brook et al., 2013). This positive feedback mechanism will be enhanced when the fragmentation threshold is
451 reached, resulting in the loss of most habitat specialist species at a landscape scale (Pardini et al., 2010). Some
452 authors have argued that since species have heterogeneous responses to habitat loss and fragmentation, and
453 biotic dispersal is limited, the importance of thresholds is restricted to local scales or even that its existence
454 is questionable (Brook et al., 2013). Fragmentation is by definition a local process that at some point
455 produces emergent phenomena over the entire landscape, even if the area considered is infinite (B. Oborny,
456 Meszéna, & Szabó, 2005). In addition, after a region's fragmentation threshold connectivity decreases, there
457 is still a large and internally well connected patch that can maintain sensitive species (A. C. Martensen,
458 Ribeiro, Banks-Leite, Prado, & Metzger, 2012). What is the time needed for these large patches to become
459 fragmented, and pose a real danger of extinction to a myriad of sensitive species? If a forest is already in
460 a fragmented state, a second critical transition from forest to non-forest could happen: the desertification
461 transition (Corrado et al., 2014). Considering the actual trends of habitat loss, and studying the dynamics
462 of non-forest patches—instead of the forest patches as we did here—the risk of this kind of transition could

463 be estimated. The simple models proposed previously could also be used to estimate if these thresholds are
464 likely to be continuous and reversible or discontinuous and often irreversible (Weissmann & Shnerb, 2016),
465 and the degree of protection (e.g. using the set-asides strategy Banks-Leite et al. (2014)) that would be
466 necessary to stop this trend.

467 The effectiveness of landscape management is related to the degree of fragmentation, and the criteria to
468 direct reforestation efforts could be focused on regions near a transition (B. Oborny et al., 2007). Regions
469 that are in an unconnected state require large efforts to recover a connected state, but regions that are near
470 a transition could be easily pushed to a connected state; feedbacks due to facilitation mechanisms might
471 help to maintain this state. Crossing the fragmentation critical point in forests could have negative effects
472 on biodiversity and ecosystem services (Haddad et al., 2015), but it could also produce feedback loops at
473 different levels of the biological hierarchy. This means that a critical transition produced at a continental
474 scale could have effects at the level of communities, food webs, populations, phenotypes and genotypes
475 (Barnosky et al., 2012). All these effects interact with climate change, thus there is a potential production of
476 cascading effects that could lead to an abrupt climate change with potentially large ecological and economic
477 impact (Alley et al., 2003).

478 Therefore, even if critical thresholds are reached only in some forest regions at a continental scale, a cascading
479 effect with global consequences could still be produced (Reyer, Rammig, Brouwers, & Langerwisch, 2015).
480 The risk of such event will be higher if the dynamics of separate continental regions are coupled (Lenton
481 & Williams, 2013). At least three of the regions defined here are considered tipping elements of the earth
482 climate system that could be triggered during this century (Lenton et al., 2008). These were defined as policy
483 relevant tipping elements so that political decisions could determine whether the critical value is reached or
484 not. Thus using the criteria proposed here could be used as a more sensitive system to evaluate the closeness
485 of a tipping point at a continental scale, but the same criteria could also be used to evaluate local problems
486 at smaller areas. Further improvements will produce quantitative predictions about the temporal horizon
487 where these critical transitions could produce significant changes in the studied systems.

488 Supporting information

489 Appendix

490 *Table S1:* Mean power-law exponent and Bootstrapped 95% confidence intervals by threshold.

491 *Table S2:* Mean power-law exponent and Bootstrapped 95% confidence intervals across thresholds by region
492 and year.

- 493 *Table S3*: Mean total patch area; largest patch S_{max} in km²; largest patch proportional to total patch area
 494 RS_{max} and 95% bootstrapped confidence interval of RS_{max} , by region and thresholds, averaged across years
- 495 *Table S4*: Model selection for distributions of fluctuation of largest patch ΔS_{max} and largest patch relative
 496 to total forest area ΔRS_{max} .
- 497 *Table S5*: Quantil regressions of the fluctuations of the largest patch vs year, for 10% and 90% quantils at
 498 different pixel thresholds.
- 499 *Table S6*: Unbiased estimation of Skewness of fluctuations of the largest patch ΔS_{max} and fluctuations
 500 relative to total forest area ΔRS_{max} .
- 501 *Figure S1*: Regions for Africa: Mainland (AF1), Madagascar (AF2).
- 502 *Figure S2*: Regions for Eurasia: Mainland (EUAS1), Japan (EUAS2), Great Britain (EUAS3).
- 503 *Figure S3*: Regions for North America: Mainland (NA1), Newfoundland (NA5).
- 504 *Figure S4*: Regions for Australia and islands: Australia mainland (OC1), New Guinea (OC2),
 505 Malaysia/Kalimantan (OC3), Sumatra (OC4), Sulawesi (OC5), New Zealand south island (OC6),
 506 Java (OC7), New Zealand north island (OC8).
- 507 *Figure S5*: Regions for South America: Tropical and subtropical forest up to Mexico (SAST1), Cuba
 508 (SAST2), South America Temperate forest (SAT1).
- 509 *Figure S6*: Regions for Southeast Asia: Mainland (SEAS1), Philippines (SEAS2).
- 510 *Figure S7*: Proportion of best models selected for patch size distributions using the Akaike criterion.
- 511 *Figure S8*: Power law exponents for forest patch distributions by year for all regions.
- 512 *Figure S9*: Average largest patch relative to total forest area RS_{max} by threshold, for all regions.
- 513 *Figure S10*: Largest patch relative to total forest area RS_{max} by year at 40% threshold, for regions with
 514 total forest area less than 10⁷ km².
- 515 *Figure S11*: Fluctuations of largest patch relative to total forest area RS_{max} for regions with total forest
 516 area less than 10⁷ km² by year and threshold.

517 Data Accessibility

- 518 Csv text file with model fits for patch size distribution, and model selection for all the regions; Gif Animations
 519 of a forest model percolation; Gif animations of largest patches; patch size files for all years and regions used

520 here; and all the R, Python and Matlab scripts are available at figshare <http://dx.doi.org/10.6084/m9.>
521 figshare.4263905.

522 Acknowledgments

523 LAS and SRD are grateful to the National University of General Sarmiento for financial support. We want to
524 thank to Jordi Bascompte, Nara Guisoni, Fernando Momo, and two anonymous reviewers for their comments
525 and discussions that greatly improved the manuscript. This work was partially supported by a grant from
526 CONICET (PIO 144-20140100035-CO).

527 References

- 528 Alley, R. B., Marotzke, J., Nordhaus, W. D., Overpeck, J. T., Peteet, D. M., Pielke, R. A., ... Wallace, J. M.
529 (2003). Abrupt Climate Change. *Science*, 299(5615), 2005–2010. Retrieved from <http://science.sciencemag.org/content/299/5615/2005.abstract>
- 530 Allington, G. R. H., & Valone, T. J. (2010). Reversal of desertification: The role of physical and chemical
531 soil properties. *Journal of Arid Environments*, 74(8), 973–977. doi:10.1016/j.jaridenv.2009.12.005
- 532 Alstott, J., Bullmore, E., & Plenz, D. (2014). powerlaw: A Python Package for Analysis of Heavy-Tailed
533 Distributions. *PLOS ONE*, 9(1), e85777. Retrieved from <https://doi.org/10.1371/journal.pone.0085777>
- 534 Angelsen, A. (2010). Policies for reduced deforestation and their impact on agricultural production. *Pro-*
535 *ceedings of the National Academy of Sciences*, 107(46), 19639–19644. doi:10.1073/pnas.0912014107
- 536 Banks-Leite, C., Pardini, R., Tambosi, L. R., Pearse, W. D., Bueno, A. A., Bruscagin, R. T., ... Metzger,
537 J. P. (2014). Using ecological thresholds to evaluate the costs and benefits of set-asides in a biodiversity
538 hotspot. *Science*, 345(6200), 1041–1045. doi:10.1126/science.1255768
- 539 Barnosky, A. D., Hadly, E. A., Bascompte, J., Berlow, E. L., Brown, J. H., Fortelius, M., ... Smith, A. B.
540 (2012). Approaching a state shift in Earth’s biosphere. *Nature*, 486(7401), 52–58. doi:10.1038/nature11018
- 541 Bascompte, J., & Solé, R. V. (1996). Habitat fragmentation and extinction threholds in spatially explicit
542 models. *Journal of Animal Ecology*, 65(4), 465–473. doi:10.2307/5781
- 543 Bazant, M. Z. (2000). Largest cluster in subcritical percolation. *Physical Review E*, 62(2), 1660–1669.
544 Retrieved from <http://link.aps.org/doi/10.1103/PhysRevE.62.1660>
- 545 Belward, A. S. (1996). *The IGBP-DIS Global 1 Km Land Cover Data Set “DISCover”: Proposal and*

- 547 *Implementation Plans : Report of the Land Recover Working Group of IGBP-DIS* (p. 61). IGBP-DIS Office.
- 548 Retrieved from <https://books.google.com.ar/books?id=qixsNAAACAAJ>
- 549 Benedetti-Cecchi, L., Tamburello, L., Maggi, E., & Bulleri, F. (2015). Experimental Perturbations Mod-
- 550 ify the Performance of Early Warning Indicators of Regime Shift. *Current Biology*, 25(14), 1867–1872.
- 551 doi:10.1016/j.cub.2015.05.035
- 552 Bestelmeyer, B. T., Duniway, M. C., James, D. K., Burkett, L. M., & Havstad, K. M. (2013). A test of
- 553 critical thresholds and their indicators in a desertification-prone ecosystem: more resilience than we thought.
- 554 *Ecology Letters*, 16, 339–345. doi:10.1111/ele.12045
- 555 Bestelmeyer, B. T., Ellison, A. M., Fraser, W. R., Gorman, K. B., Holbrook, S. J., Laney, C. M., ... Sharma,
- 556 S. (2011). Analysis of abrupt transitions in ecological systems. *Ecosphere*, 2(12), 129. doi:10.1890/ES11-
- 557 00216.1
- 558 Boettiger, C., & Hastings, A. (2012). Quantifying limits to detection of early warning for critical transitions.
- 559 *Journal of the Royal Society Interface*, 9(75), 2527–2539. doi:10.1098/rsif.2012.0125
- 560 Bonan, G. B. (2008). Forests and Climate Change: forcings, Feedbacks, and the Climate Benefits of Forests.
- 561 *Science*, 320(5882), 1444–1449. doi:10.1126/science.1155121
- 562 Botet, R., & Ploszajczak, M. (2004). Correlations in Finite Systems and Their Universal Scaling Properties.
- 563 In K. Morawetz (Ed.), *Nonequilibrium physics at short time scales: Formation of correlations* (pp. 445–466).
- 564 Berlin Heidelberg: Springer-Verlag.
- 565 Brook, B. W., Ellis, E. C., Perring, M. P., Mackay, A. W., & Blomqvist, L. (2013). Does the terrestrial
- 566 biosphere have planetary tipping points? *Trends in Ecology & Evolution*. doi:10.1016/j.tree.2013.01.016
- 567 Burnham, K., & Anderson, D. R. (2002). *Model selection and multi-model inference: A practical information-*
- 568 *theoretic approach* (2nd. ed., p. 512). New York: Springer-Verlag.
- 569 Canfield, D. E., Glazer, A. N., & Falkowski, P. G. (2010). The Evolution and Future of Earth's Nitrogen
- 570 Cycle. *Science*, 330(6001), 192–196. doi:10.1126/science.1186120
- 571 Carpenter, S. R., Cole, J. J., Pace, M. L., Batt, R., Brock, W. A., Cline, T., ... Weidel, B. (2011).
- 572 Early Warnings of Regime Shifts: A Whole-Ecosystem Experiment. *Science*, 332(6033), 1079–1082.
- 573 doi:10.1126/science.1203672
- 574 Clauset, A., Shalizi, C., & Newman, M. (2009). Power-Law Distributions in Empirical Data. *SIAM Review*,

- 575 51(4), 661–703. doi:10.1137/070710111
- 576 Corrado, R., Cherubini, A. M., & Pennetta, C. (2014). Early warning signals of desertification transitions
577 in semiarid ecosystems. *Physical Review E - Statistical, Nonlinear, and Soft Matter Physics*, 90(6), 62705.
578 doi:10.1103/PhysRevE.90.062705
- 579 Crawley, M. J. (2012). *The R Book* (2nd. ed., p. 1076). Hoboken, NJ, USA: Wiley.
- 580 Crowther, T. W., Glick, H. B., Covey, K. R., Bettigole, C., Maynard, D. S., Thomas, S. M., ... Bradford, M.
581 A. (2015). Mapping tree density at a global scale. *Nature*, 525(7568), 201–205. doi:10.1038/nature14967
- 582 Dai, L., Vorselen, D., Korolev, K. S., & Gore, J. (2012). Generic Indicators for Loss of Resilience Before a
583 Tipping Point Leading to Population Collapse. *Science*, 336(6085), 1175–1177. doi:10.1126/science.1219805
- 584 DiMiceli, C., Carroll, M., Sohlberg, R., Huang, C., Hansen, M., & Townshend, J. (2015). Annual Global Au-
585 tomated MODIS Vegetation Continuous Fields (MOD44B) at 250 m Spatial Resolution for Data Years Begin-
586 ning Day 65, 2000 - 2014, Collection 051 Percent Tree Cover, University of Maryland, College Park, MD, USA.
587 Retrieved from https://lpdaac.usgs.gov/dataset{_}discovery/modis/modis{_}products{_}table/mod44b
- 588 Drake, J. M., & Griffen, B. D. (2010). Early warning signals of extinction in deteriorating environments.
589 *Nature*, 467(7314), 456–459. doi:10.1038/nature09389
- 590 Efron, B., & Tibshirani, R. J. (1994). *An Introduction to the Bootstrap* (p. 456). New York: Taylor &
591 Francis. Retrieved from <https://books.google.es/books?id=gLlpIUXRntoC>
- 592 Filotas, E., Parrott, L., Burton, P. J., Chazdon, R. L., Coates, K. D., Coll, L., ... Messier, C. (2014). Viewing
593 forests through the lens of complex systems science. *Ecosphere*, 5(January), 1–23. doi:10.1890/ES13-00182.1
- 594 Foley, J. A., Ramankutty, N., Brauman, K. A., Cassidy, E. S., Gerber, J. S., Johnston, M., ... Zaks, D. P. M.
595 (2011). Solutions for a cultivated planet. *Nature*, 478(7369), 337–342. doi:10.1038/nature10452
- 596 Folke, C., Jansson, Å., Rockström, J., Olsson, P., Carpenter, S. R., Iii, F. S. C., ... Westley, F. (2011).
597 Reconnecting to the Biosphere. *AMBIO*, 40(7), 719–738. doi:10.1007/s13280-011-0184-y
- 598 Fung, T., O'Dwyer, J. P., Rahman, K. A., Fletcher, C. D., & Chisholm, R. A. (2016). Reproducing static
599 and dynamic biodiversity patterns in tropical forests: the critical role of environmental variance. *Ecology*,
600 97(5), 1207–1217. doi:10.1890/15-0984.1
- 601 Gardner, R. H., & Urban, D. L. (2007). Neutral models for testing landscape hypotheses. *Landscape Ecology*,
602 22(1), 15–29. doi:10.1007/s10980-006-9011-4
- 603 Gastner, M. T., Oborny, B., Zimmermann, D. K., & Pruessner, G. (2009). Transition from Connected

- 604 to Fragmented Vegetation across an Environmental Gradient: Scaling Laws in Ecotone Geometry. *The*
605 *American Naturalist*, 174(1), E23–E39. doi:10.1086/599292
- 606 Gauthier, S., Bernier, P., Kuuluvainen, T., Shvidenko, A. Z., & Schepaschenko, D. G. (2015). Boreal forest
607 health and global change. *Science*, 349(6250), 819 LP–822. Retrieved from <http://science.sciencemag.org/content/349/6250/819.abstract>
- 609 Gilman, S. E., Urban, M. C., Tewksbury, J., Gilchrist, G. W., & Holt, R. D. (2010). A framework
610 for community interactions under climate change. *Trends in Ecology & Evolution*, 25(6), 325–331.
611 doi:10.1016/j.tree.2010.03.002
- 612 Goldstein, M. L., Morris, S. A., & Yen, G. G. (2004). Problems with fitting to the power-law distri-
613 bution. *The European Physical Journal B - Condensed Matter and Complex Systems*, 41(2), 255–258.
614 doi:10.1140/epjb/e2004-00316-5
- 615 Haddad, N. M., Brudvig, L. a., Clobert, J., Davies, K. F., Gonzalez, A., Holt, R. D., ... Townshend, J. R.
616 (2015). Habitat fragmentation and its lasting impact on Earth's ecosystems. *Science Advances*, 1(2), 1–9.
617 doi:10.1126/sciadv.1500052
- 618 Hansen, M. C., Potapov, P. V., Moore, R., Hancher, M., Turubanova, S. A., Tyukavina, A., ... Townshend,
619 J. R. G. (2013). High-Resolution Global Maps of 21st-Century Forest Cover Change. *Science*, 342(6160),
620 850–853. doi:10.1126/science.1244693
- 621 Hansen, M., Potapov, P., Margono, B., Stehman, S., Turubanova, S., & Tyukavina, A. (2014). Response
622 to Comment on “High-resolution global maps of 21st-century forest cover change”. *Science*, 344(6187), 981.
623 doi:10.1126/science.1248817
- 624 Hantson, S., Pueyo, S., & Chuvieco, E. (2015). Global fire size distribution is driven by human impact and
625 climate. *Global Ecology and Biogeography*, 24(1), 77–86. doi:10.1111/geb.12246
- 626 Harris, T. E. (1974). Contact interactions on a lattice. *The Annals of Probability*, 2, 969–988.
- 627 Hartigan, J. A., & Hartigan, P. M. (1985). The Dip Test of Unimodality. *The Annals of Statistics*, 13(1),
628 70–84. Retrieved from <http://www.jstor.org/stable/2241144>
- 629 Hastings, A., & Wysham, D. B. (2010). Regime shifts in ecological systems can occur with no warning.
630 *Ecology Letters*, 13(4), 464–472. doi:10.1111/j.1461-0248.2010.01439.x
- 631 He, F., & Hubbell, S. (2003). Percolation Theory for the Distribution and Abundance of Species. *Physical*

- 632 *Review Letters*, 91(19), 198103. doi:10.1103/PhysRevLett.91.198103
- 633 Heffernan, J. B., Soranno, P. A., Angilletta, M. J., Buckley, L. B., Gruner, D. S., Keitt, T. H., ... Weathers, K. C. (2014). Macrosystems ecology: understanding ecological patterns and processes at continental scales.
- 634 *Frontiers in Ecology and the Environment*, 12(1), 5–14. doi:10.1890/130017
- 635 Hinrichsen, H. (2000). Non-equilibrium critical phenomena and phase transitions into absorbing states.
- 636 *Advances in Physics*, 49(7), 815–958. doi:10.1080/00018730050198152
- 637 Hirota, M., Holmgren, M., Nes, E. H. V., & Scheffer, M. (2011). Global Resilience of Tropical Forest and Savanna to Critical Transitions. *Science*, 334(6053), 232–235. doi:10.1126/science.1210657
- 638 Irvine, M. A., Bull, J. C., & Keeling, M. J. (2016). Aggregation dynamics explain vegetation patch-size distributions. *Theoretical Population Biology*, 108, 70–74. doi:10.1016/j.tpb.2015.12.001
- 639 Keitt, T. H., Urban, D. L., & Milne, B. T. (1997). Detecting critical scales in fragmented landscapes.
- 640 *Conservation Ecology*, 1(1), 4. Retrieved from <http://www.ecologyandsociety.org/vol1/iss1/art4/>
- 641 Kéfi, S., Guttal, V., Brock, W. A., Carpenter, S. R., Ellison, A. M., Livina, V. N., ... Dakos, V. (2014). Early Warning Signals of Ecological Transitions: Methods for Spatial Patterns. *PLoS ONE*, 9(3), e92097. doi:10.1371/journal.pone.0092097
- 642 Kéfi, S., Rietkerk, M., Alados, C. L., Pueyo, Y., Papanastasis, V. P., ElAich, A., & Ruiter, P. C. de. (2007). Spatial vegetation patterns and imminent desertification in Mediterranean arid ecosystems. *Nature*, 449(7159), 213–217. doi:10.1038/nature06111
- 643 Kitzberger, T., Aráoz, E., Gowda, J. H., Mermoz, M., & Morales, J. M. (2012). Decreases in Fire Spread Probability with Forest Age Promotes Alternative Community States, Reduced Resilience to Climate Variability and Large Fire Regime Shifts. *Ecosystems*, 15(1), 97–112. doi:10.1007/s10021-011-9494-y
- 644 Koenker, R. (2016). quantreg: Quantile Regression. Retrieved from <http://cran.r-project.org/package=quantreg>
- 645 Lasco, R. D., Pulhin, F. B., Cruz, R. V. O., Pulhin, J. M., Roy, S. S. N., & Sanchez, P. A. J. (2008). Forest responses to changing rainfall in the Philippines. In N. Leary, C. Conde, & J. Kulkarni (Eds.), *Climate change and vulnerability* (pp. 49–66). London: Earthscan. Retrieved from <http://gen.lib.rus.ec/book/index.php?md5=AD313B13E05C9D61A9EC1EE2E73A91FB>
- 646 Leibold, M. A., & Norberg, J. (2004). Biodiversity in metacommunities: Plankton as complex adaptive

- systems? *Limnology and Oceanography*, 49(4, part 2), 1278–1289. doi:10.4319/lo.2004.49.4_part_2.1278
- Lenton, T. M., & Williams, H. T. P. (2013). On the origin of planetary-scale tipping points. *Trends in Ecology & Evolution*, 28(7), 380–382. doi:10.1016/j.tree.2013.06.001
- Lenton, T. M., Held, H., Kriegler, E., Hall, J. W., Lucht, W., Rahmstorf, S., & Schellnhuber, H. J. (2008). Tipping elements in the Earth's climate system. *Proceedings of the National Academy of Sciences*, 105(6), 1786–1793. doi:10.1073/pnas.0705414105
- Limpert, E., Stahel, W. A., & Abbt, M. (2001). Log-normal Distributions across the Sciences: Keys and CluesOn the charms of statistics, and how mechanical models resembling gambling machines offer a link to a handy way to characterize log-normal distributions, which can provide deeper insight into var. *BioScience*, 51(5), 341–352. Retrieved from [http://dx.doi.org/10.1641/0006-3568\(2001\)051\[0341:LNDATS\]2.0.CO](http://dx.doi.org/10.1641/0006-3568(2001)051[0341:LNDATS]2.0.CO)
- Loehle, C., Li, B.-L., & Sundell, R. C. (1996). Forest spread and phase transitions at forest-prairie ecotones in Kansas, U.S.A. *Landscape Ecology*, 11(4), 225–235.
- Malhi, Y., Gardner, T. A., Goldsmith, G. R., Silman, M. R., & Zelazowski, P. (2014). Tropical Forests in the Anthropocene. *Annual Review of Environment and Resources*, 39(1), 125–159. doi:10.1146/annurev-environ-030713-155141
- Manor, A., & Shnerb, N. M. (2008). Origin of pareto-like spatial distributions in ecosystems. *Physical Review Letters*, 101(26), 268104. doi:10.1103/PhysRevLett.101.268104
- Martensen, A. C., Ribeiro, M. C., Banks-Leite, C., Prado, P. I., & Metzger, J. P. (2012). Associations of Forest Cover, Fragment Area, and Connectivity with Neotropical Understory Bird Species Richness and Abundance. *Conservation Biology*, 26(6), 1100–1111. doi:10.1111/j.1523-1739.2012.01940.x
- McKenzie, D., & Kennedy, M. C. (2012). Power laws reveal phase transitions in landscape controls of fire regimes. *Nat Commun*, 3, 726. Retrieved from <http://dx.doi.org/10.1038/ncomms1731> http://www.nature.com/ncomms/journal/v3/n3/suppinfo/ncomms1731{_\}S1.html
- Mitchell, M. G. E., Suarez-Castro, A. F., Martinez-Harms, M., Maron, M., McAlpine, C., Gaston, K. J., ... Rhodes, J. R. (2015). Reframing landscape fragmentation's effects on ecosystem services. *Trends in Ecology & Evolution*, 30(4), 190–198. doi:10.1016/j.tree.2015.01.011
- Naito, A. T., & Cairns, D. M. (2015). Patterns of shrub expansion in Alaskan arctic river corridors suggest phase transition. *Ecology and Evolution*, 5(1), 87–101. doi:10.1002/ece3.1341
- Newman, M. E. J. (2005). Power laws, Pareto distributions and Zipf's law. *Contemporary Physics*, 46(5),

- 689 323–351. doi:10.1080/00107510500052444
- 690 Oborny, B., Meszéna, G., & Szabó, G. (2005). Dynamics of Populations on the Verge of Extinction. *Oikos*,
691 109(2), 291–296. Retrieved from <http://www.jstor.org/stable/3548746>
- 692 Oborny, B., Szabó, G., & Meszéna, G. (2007). Survival of species in patchy landscapes: percolation in
693 space and time. In *Scaling biodiversity* (pp. 409–440). Cambridge University Press. Retrieved from <http://dx.doi.org/10.1017/CBO9780511814938.022>
- 695 Ochoa-Quintero, J. M., Gardner, T. A., Rosa, I., de Barros Ferraz, S. F., & Sutherland, W. J. (2015).
696 Thresholds of species loss in Amazonian deforestation frontier landscapes. *Conservation Biology*, 29(2),
697 440–451. doi:10.1111/cobi.12446
- 698 Ódor, G. (2004). Universality classes in nonequilibrium lattice systems. *Reviews of Modern Physics*, 76(3
699 I), 663–724. doi:10.1103/RevModPhys.76.663
- 700 Pardini, R., Bueno, A. de A., Gardner, T. A., Prado, P. I., & Metzger, J. P. (2010). Beyond the Fragmen-
701 tation Threshold Hypothesis: Regime Shifts in Biodiversity Across Fragmented Landscapes. *PLoS ONE*,
702 5(10), e13666. doi:10.1371/journal.pone.0013666
- 703 Potapov, P., Hansen, M. C., Stehman, S. V., Loveland, T. R., & Pittman, K. (2008). Combining MODIS
704 and Landsat imagery to estimate and map boreal forest cover loss. *Remote Sensing of Environment*, 112(9),
705 3708–3719. doi:<https://doi.org/10.1016/j.rse.2008.05.006>
- 706 Potapov, P., Yaroshenko, A., Turubanova, S., Dubinin, M., Laestadius, L., Thies, C., ... Zhuravleva, I. (2008).
707 Mapping the world's intact forest landscapes by remote sensing. *Ecology and Society*, 13(2).
- 708 Prishchepov, A. V., Müller, D., Dubinin, M., Baumann, M., & Radeloff, V. C. (2013). Determinants
709 of agricultural land abandonment in post-Soviet European Russia. *Land Use Policy*, 30(1), 873–884.
710 doi:<https://doi.org/10.1016/j.landusepol.2012.06.011>
- 711 Pueyo, S., de Alencastro Graça, P. M. L., Barbosa, R. I., Cots, R., Cardona, E., & Fearnside, P. M. (2010).
712 Testing for criticality in ecosystem dynamics: the case of Amazonian rainforest and savanna fire. *Ecology
713 Letters*, 13(7), 793–802. doi:10.1111/j.1461-0248.2010.01497.x
- 714 R Core Team. (2015). R: A Language and Environment for Statistical Computing. Vienna, Austria: R
715 Foundation for Statistical Computing. Retrieved from <http://www.r-project.org/>
- 716 Reyer, C. P. O., Rammig, A., Brouwers, N., & Langerwisch, F. (2015). Forest resilience, tipping points and

- 717 global change processes. *Journal of Ecology*, 103(1), 1–4. doi:10.1111/1365-2745.12342
- 718 Rockstrom, J., Steffen, W., Noone, K., Persson, A., Chapin, F. S., Lambin, E. F., ... Foley, J. A. (2009). A
719 safe operating space for humanity. *Nature*, 461(7263), 472–475. Retrieved from <http://dx.doi.org/10.1038/461472a>
- 721 Rooij, M. M. J. W. van, Nash, B., Rajaraman, S., & Holden, J. G. (2013). A Fractal Approach to Dynamic
722 Inference and Distribution Analysis. *Frontiers in Physiology*, 4(1). doi:10.3389/fphys.2013.00001
- 723 Rudel, T. K., Coomes, O. T., Moran, E., Achard, F., Angelsen, A., Xu, J., & Lambin, E. (2005). Forest
724 transitions: towards a global understanding of land use change. *Global Environmental Change*, 15(1), 23–31.
725 doi:<https://doi.org/10.1016/j.gloenvcha.2004.11.001>
- 726 Saravia, L. A., & Momo, F. R. (2017). Biodiversity collapse and early warning indicators in
727 a spatial phase transition between neutral and niche communities. *PeerJ PrePrints*, 5, e1589v4.
728 doi:10.7287/peerj.preprints.1589v3
- 729 Scanlon, T. M., Caylor, K. K., Levin, S. A., & Rodriguez-iturbe, I. (2007). Positive feedbacks promote
730 power-law clustering of Kalahari vegetation. *Nature*, 449(September), 209–212. doi:10.1038/nature06060
- 731 Scheffer, M., Bascompte, J., Brock, W. A., Brovkin, V., Carpenter, S. R., Dakos, V., ... Sugihara, G. (2009).
732 Early-warning signals for critical transitions. *Nature*, 461(7260), 53–59. doi:10.1038/nature08227
- 733 Scheffer, M., Walker, B., Carpenter, S., Foley, J. a, Folke, C., & Walker, B. (2001). Catastrophic shifts in
734 ecosystems. *Nature*, 413(6856), 591–596. doi:10.1038/35098000
- 735 Seidler, T. G., & Plotkin, J. B. (2006). Seed Dispersal and Spatial Pattern in Tropical Trees. *PLoS Biology*,
736 4(11), e344. doi:10.1371/journal.pbio.0040344
- 737 Sexton, J. O., Noojipady, P., Song, X.-P., Feng, M., Song, D.-X., Kim, D.-H., ... Townshend, J. R.
738 (2015). Conservation policy and the measurement of forests. *Nature Climate Change*, 6(2), 192–196.
739 doi:10.1038/nclimate2816
- 740 Sexton, J. O., Song, X.-P., Feng, M., Noojipady, P., Anand, A., Huang, C., ... Townshend, J. R. (2013).
741 Global, 30-m resolution continuous fields of tree cover: Landsat-based rescaling of MODIS vegetation con-
742 tinuous fields with lidar-based estimates of error. *International Journal of Digital Earth*, 6(5), 427–448.
743 doi:10.1080/17538947.2013.786146
- 744 Solé, R. V. (2011). *Phase Transitions* (p. 223). Princeton University Press. Retrieved from https://books.google.com/books?id=KUWzDwAAQBAJ&pg=PA223&lpg=PA223&dq=phase+transitions+R+V+Sole&source=bl&ots=ZBxGKqfCgk&sig=9yfOOGdLcIwzrJFmzJLJLJLJL&hl=en&sa=X&redir_esc=y

- 745 google.com.ar/books?id=8RcLuv-Ll2kC
- 746 Solé, R. V., & Bascompte, J. (2006). *Self-organization in complex ecosystems* (p. 373). New Jersey, USA.:
747 Princeton University Press. Retrieved from <http://books.google.com.ar/books?id=v4gpGH6Gv68C>
- 748 Solé, R. V., Alonso, D., & Mckane, A. (2002). Self-organized instability in complex ecosystems. *Philosophical Transactions of the Royal Society of London. Series B, Biological Sciences*, 357(May), 667–681.
749
750 doi:10.1098/rstb.2001.0992
- 751 Solé, R. V., Alonso, D., & Saldaña, J. (2004). Habitat fragmentation and biodiversity collapse in neutral
752 communities. *Ecological Complexity*, 1(1), 65–75. doi:10.1016/j.ecocom.2003.12.003
- 753 Solé, R. V., Bartumeus, F., & Gamarra, J. G. P. (2005). Gap percolation in rainforests. *Oikos*, 110(1),
754 177–185. doi:10.1111/j.0030-1299.2005.13843.x
- 755 Staal, A., Dekker, S. C., Xu, C., & Nes, E. H. van. (2016). Bistability, Spatial Interaction, and the
756 Distribution of Tropical Forests and Savannas. *Ecosystems*, 19(6), 1080–1091. doi:10.1007/s10021-016-0011-
757 1
- 758 Stauffer, D., & Aharony, A. (1994). *Introduction To Percolation Theory* (p. 179). London: Taylor & Francis.
- 759 Vasilakopoulos, P., & Marshall, C. T. (2015). Resilience and tipping points of an exploited fish population
760 over six decades. *Global Change Biology*, 21(5), 1834–1847. doi:10.1111/gcb.12845
- 761 Verbesselt, J., Umlauf, N., Hirota, M., Holmgren, M., Van Nes, E. H., Herold, M., ... Scheffer, M. (2016). Re-
762 motely sensed resilience of tropical forests. *Nature Climate Change*, 1(September). doi:10.1038/nclimate3108
- 763 Villa Martín, P., Bonachela, J. A., & Muñoz, M. A. (2014). Quenched disorder forbids discontinuous
764 transitions in nonequilibrium low-dimensional systems. *Physical Review E*, 89(1), 12145. Retrieved from
765 <https://link.aps.org/doi/10.1103/PhysRevE.89.012145>
- 766 Villa Martín, P., Bonachela, J. A., Levin, S. A., & Muñoz, M. A. (2015). Eluding catastrophic shifts.
767 *Proceedings of the National Academy of Sciences*, 112(15), E1828–E1836. doi:10.1073/pnas.1414708112
- 768 Viña, A., McConnell, W. J., Yang, H., Xu, Z., & Liu, J. (2016). Effects of conservation policy on China's
769 forest recovery. *Science Advances*, 2(3), e1500965. Retrieved from <http://advances.sciencemag.org/content/2/3/e1500965.abstract>
- 770
771 Vuong, Q. H. (1989). Likelihood Ratio Tests for Model Selection and Non-Nested Hypotheses. *Econometrica*,
772 57(2), 307–333. doi:10.2307/1912557
- 773 Weerman, E. J., Van Belzen, J., Rietkerk, M., Temmerman, S., Kéfi, S., Herman, P. M. J., & Koppell, J. V.

- 774 de. (2012). Changes in diatom patch-size distribution and degradation in a spatially self-organized intertidal
775 mudflat ecosystem. *Ecology*, 93(3), 608–618. doi:10.1890/11-0625.1
- 776 Weissmann, H., & Shnerb, N. M. (2016). Predicting catastrophic shifts. *Journal of Theoretical Biology*, 397,
777 128–134. doi:10.1016/j.jtbi.2016.02.033
- 778 Wuyts, B., Champneys, A. R., & House, J. I. (2017). Amazonian forest-savanna bistability and human
779 impact. *Nature Communications*, 8(May), 15519. doi:10.1038/ncomms15519
- 780 Xu, C., Hantson, S., Holmgren, M., Nes, E. H. van, Staal, A., & Scheffer, M. (2016). Remotely sensed
781 canopy height reveals three pantropical ecosystem states. *Ecology*, 97(9), 2518–2521. doi:10.1002/ecy.1470
- 782 Zhang, J. Y., Wang, Y., Zhao, X., Xie, G., & Zhang, T. (2005). Grassland recovery by protection from
783 grazing in a semi-arid sandy region of northern China. *New Zealand Journal of Agricultural Research*, 48(2),
784 277–284. doi:10.1080/00288233.2005.9513657
- 785 Zinck, R. D., & Grimm, V. (2009). Unifying wildfire models from ecology and statistical physics. *The
786 American Naturalist*, 174(5), E170–85. doi:10.1086/605959